AN MO CAVITY MODEL OF ENZYME CATALYSIS: SEMIEMPIRICAL CALCULATIONS OF REACTION COURSES OF ACETALDEHYDE REDUCTION AND ETHANOL OXIDATION BY AN NAD MODEL

Jiří KRECHL and Josef KUTHAN

Department of Organic Chemistry, Prague Institute of Chemical Technology, 166 28 Prague 6

Received February 18, 1988
Accepted May 3, 1988

General suggestions concerning the possibility to interpret the elementary reaction steps in biocatalytic processes, as if proceeding in pseudovacuum of a protein cavity, have been presented. The approach is illustrated by MNDO investigation of the interaction of 1-methyl-1,4-dihydronicotinamide (*II*) with acetaldehyde or its protonated species *Ia* and *Ib*, respectively. The pre-activation step *Ia* → *Ib* has been shown to accelerate the interconversion of substrate *Ib* into ethanol and 3-aminocarbonylpyridinium (*V*) more effectively than a subsequent protonation of the possible 1,6-dihydropyridine intermediate *III* arising from *Ia* and *II*. The opposite reaction path of *V* with ethanol and ethoxide is also being examined.

Regardless of the great complexity of enzymatic reactions the number of chemical calculations on this topic have been gradually increasing. In addition to several very extensive calculations[1,2], tending to the explicit inclusion of the whole or substantial part of a given protein molecule into the theoretical treatment, a large number of MO investigations based on simplified model systems has been published in literature (e.g. refs[3,4]). In view of respect to the role of the theory in general, as well as of quantum chemistry at appropriate applications in the development of modern chemical thinking, the initially mentioned oversophisticated approach to biocatalysis because of its cost and technical limitations may hardly be used effectively.

The second mentioned simplified approach that models the behavior of a substrate and cofactor molecules as independently interreacting species under implicite consideration of enzyme surroundings seems to be more promising in the discovery of new generalizable interrelations among various enzymatic processes. Although the majority of authors intuitively accept the suggestion that their model simplified MO studies, for example, on the reaction between a coenzyme and a substrate[5], involves certain important features of general biocatalysis, no attempts have been made to justify the theoretical results. Only recently, have Tapia et al.[6–8] treated the justification of the simplified MO approach more precisely mainly in connection with novel excellent X-ray structural studies on alcohol dehydrogenase[9].

In this communication we attempt to extend Tapia's approach from static to dynamic behaviour of the reacting system as changes within a Cavity Model of Enzymatic Catalysis (CMEC), we suggest that a part of biocatalytic processes may be divided into elementary steps. Those steps may be treated as if proceeding non-enzymaticaly in pseudovacuum[10]. The procedure is illustrated for a reaction step simulating the key stage of enzymatically catalyzed alcohol fermentation (*A*):

$$NADH + CH_3CHO + H^+ \overset{\text{enzyme}}{\rightleftharpoons} NAD^+ + CH_3CH_2OH\,. \qquad (A)$$

CALCULATIONS

All numerical calculations were carried out using the standard MNDO program[11] with automatic procedure searching minima on a potential hypersurface[12,13]. Because of large scale calculations we were forced to use the semiempirical quantum chemical method with an excellent optimization procedure and quick convergence of the SCF problem. On the other hand, these advantages are ballanced by the fact that the interpretation of obtained results may be treated only qualitatively. But this extensive mapping of alternative reaction paths enables us to select critical points and calculate them on a more sophisticated nonempirical level. Attempts to do so are already under progress.

RESULTS AND DISCUSSION

Every enzymatic reaction may be divided into at least three characteristic stages: (i) transfer of interacting partners (substrates, cofactors) to a macromolecular protein (enzyme), (ii) chemical interaction of the partners transforming a given substrate into the corresponding product within the protein environment and (iii) transfer of product and possibly cofactor molecules from the protein. Both transfer processes (i) and (iii) as well as conformational changes in protein macromolecule evoked by the interaction (ii) can hardly be investigated by current quantum chemical methods owing to their statistical and structural complexity. On the other hand, various interesting details concerning this stage (ii) can be understood by MO treatments which involve a non-statistical number of models of chemical particles.

Cavity Model of Enzymatic Catalysis (CMEC) *and Its Limitations*

In order to adopt usual quantum chemical models enabling the interpretation and prediction of significant aspects in the stage (ii), a generalized model of the microscopic interacting system in a protein macromolecule ought to be developed. Two important circumstances might be taken into account in this connection: Firstly, the protein

surroundings eliminate solvent effects preventing the solvent molecules to enter boundlessly an active site of the enzyme. Secondly, only a definite number of amino acid residue creates the background of the cavital reaction space.

The following conclusion may be drawn from the well known facts: Every interconversion between substrate and cofactor in the active site proceeds similar to the gas phase and is additionally facilitated with a part of internal electrostatic field of the enzyme macromolecule. In fact, these ideas are often accepted and implicitly exploited in current MO calculations related to biocatalysis. We believe that a general quantum chemical cavity model, shown in Fig. 1, may unify current theoretical investigations of microscopic processes in biocatalysis. The model exclusively refers to the active site of a given enzyme in which the conversion of desolvated substrate S into product P takes place with the participation of cofactor C. The reacting system is thought to be surrounded by an enzyme macromolecule E bearing substrate and cofactor binding sites BS and BC, respectively.

For further considerations it seems of importance that during the chemical transformation no mass transfer from the closed cavital system of reactants to its surroundings or vice versa takes place The assumed CMEC can theoretically be treated as a stationary state while using the supermolecule approach on the basis of the time-independent Schrödinger equation

$$\mathbf{H}_{CM}\Psi_{CM} = E_{CM}\Psi_{CM}\,, \tag{1}$$

where index CM denotes that Hamiltonian, wave function as well as energy concern the cavity model. Various levels of sophistication of Eq. (*1*) may be considered to physically describe the situation in Fig. 1. Thus, for the starting complex – situation

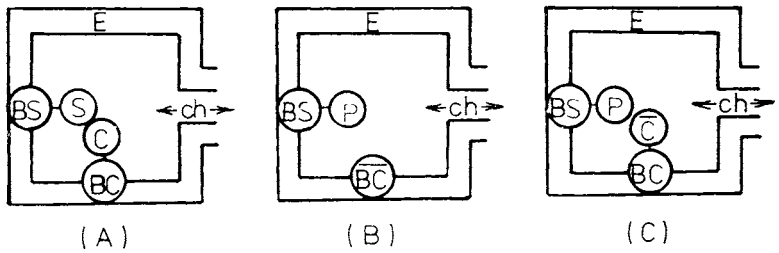

FIG. 1

Cavity model of enzymatic catalysis. (A) enzyme–substrate–cofactor complex; (B) enzyme–product complex; C enzyme–product–cofactor complex. Symbols: S substrate, P product, C cofactor, $\overline{C}$ modified cofactor, BS substrate binding site, BC cofactor binding site, $\overline{BC}$ modified cofactor binding site, ch channel transferring S, P and C molecules, E enzyme

(A) – the Hamiltonian may be written as follows:

$$\mathbf{H}_{CM} = \mathbf{H}_S + \mathbf{H}_C + \mathbf{H}_{BS} + \mathbf{H}_{BC} + \mathbf{H}_E \,. \qquad (2)$$

The right side terms $\mathbf{H}_S$ to $\mathbf{H}_{BC}$ in Eq. (*2*) are to be easily defined as Hamiltonians for MO models of individual molecules, e.g. of substrate S, cofactor C as well as of binding site components BS and BC. On the other hand, the last term $\mathbf{H}_E$ expressing environmental effects of the enzyme molecule may be treated only approximately on the basis of certain simplifications. The perturbational approach consists in the calculation of the term as an electrostatic field contribution to the hamiltonians of individual reactants and has in fact been used by several authors (e.g. ref.[14]). The variation method may alternatively be applied approximating the term $\mathbf{H}_E$ by a set of Hamiltonians derived from speculatively chosen amino acid residues or their simplified molecules[2]. Analogously to the starting complex (A) (Fig. 1) also the final complexes (B) or (C) may theoretically be treated using similar expansions of Hamiltonian $\mathbf{H}_{CM}$ like in Eq. *2*.

Minimizing the energies of the corresponding CMECs the MO models of starting and final complexes were established[15,16]. A further development ought to involve successive variations of certain geometrical parameters related to reasonable reaction coordinates. Other geometrical degrees of freedom except the reaction coordinate are optimized within every calculation step. Thus obtainment of information on experimentally hardly accessible changes of energy as well as of molecular and electronic structures during the microprocess S → P becomes possible.

Any use of CMEC will apparently be limited to enzymes in which the reaction cavity is large enough to allow a sufficient part of independent vibronic movements of reactants. Consequently, the conversion S → P in fact proceeds in pseudovacuum to a certain extent resembling a gas phase reaction of very diluted particles. On the other hand, the CMEC might be inadequate for other enzymes where the cavity is too small, the vibronic modes are strongly coupled and the effect of surroundings E in Fig. 1 resembles more a solid state reaction. In such cases a modification of the CMEC into perhaps a matrix model will probably be justified.

Application of the CMEC *to* NAD^+–NADH *Dependent Enzymatic Reactions*

Our current interest in the above titled biocatalyzed processes led us to specify in Fig. 1 complexes (A) and (C) so that C = NAD^+ and $\bar{C}$ = NADH for oxidative conversions or C = NADH and $\bar{C}$ = NAD^+ for reductive conversions described by Eq. (*A*). Further simplifications were used to make our MNDO calculations effective. Instead of the complete molecules NADH/NAD^+ only their simple bioorganic models *II* and *V* were considered as reducing or oxidizing agents, respectively. BC was thus treated only implicitly as a methyl moiety of the coenzyme model.

In the following paragraph examination of the Eq. (*A*) proceeding to the right will be presented. In order to understand the effect of substrate activation, two series of alternative calculations were performed – one using complete neglect of BS and the other involving protonated substrate $CH_3CHOH^{(+)}$ as a model of the coordination to zinc in real BS (cf.[9]). Our illustrative calculations still lack the inclusion of $\mathbf{H}_E$ from Eq. (*2*). This expansion will be subject of further study. Individual components of so simplified CMEC are shown in Fig. 2.

Reaction of 1-*Methyl*-1,4-*dihydronicotinamide with Acetaldehyde*

The strategy of our MO calculation, as we have recently presented in a preliminary communication[17], is based on MNDO model of the starting complex (A) (Fig. 2, *Ia–II*) which is successively transformed into MNDO model of analogous complex of products by variation of $C_{21}...H_{17}$ distance. We issued from supermolecule *Ia–II* of the same nuclear configuration as of that calculated previously[18–20] on the basis of the rigid rotators method. Because of diastereoisomerism in the system *Ia–II* the alternative was used in which pro(R) hydrogen centre H_{17} faces toward re-side of the carbonyl group C_{21}—O_{23} as it corresponds to the particular arrangement in the native horse liver alcohol dehydrogenase (EC 1.1.1.1). Then the entire 75 geometrical degrees of freedom of the system were optimized (Table I).

In the following procedure distance $C_{21}...H_{17}$ has been successively shortened in steps 20 to 10 pm starting from the distance 200 pm (point A_1 on the reaction path)

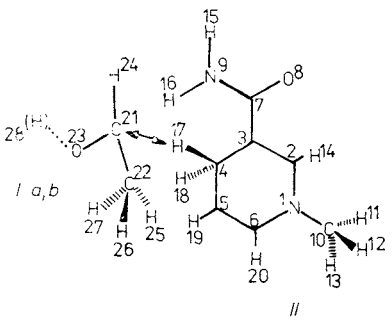

FIG. 2

Numbering of the studied system *Ia, b–II*. *Ia* acetaldehyde, *Ib* O-protonated acetaldehyde, *II* 1-methyl-1,4-dihydronicotinamide

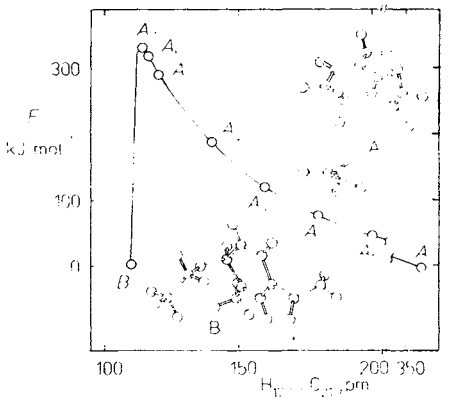

FIG. 3

Dependence of MNDO energy on distance between centres H_{17} and C_{21} in supermolecule *Ia–II*

and after every step the reacting system was optimized with respect to other degrees of freedom except the fixed distance. Fig. 3 shows that energy of the system gradually increases up to the value of the fixed distance near 114 pm (point A_7) and then steeply falls to an apparent minimum of about 112 pm (point B) where nuclear configuration is undoubtedly that approximating a complex of products. In optimizing it, however, with respect to all 75 geometrical degrees of freedom the resulting optimal nuclear configuration B lays only 4 kJ mol^{-1} above that of starting complex (A), thus suggesting that the transformation (A) → (B) might be only slightly endo-

TABLE I

Nuclear coordinates for optimal configuration of supermolecule *Ia–II* (A)

Atoms				Bond length, pm	Bond angle, °	Dihedral angle, °
I	J	K	L	J—I	K—J—I	L—K—J—I
2	1			140·49		
3	2	1		136·50	122·126	
4	3	2	1	151·59	121·836	−3·603
5	4	3	2	150·31	112·062	2·419
6	5	4	3	135·42	123·244	−0·687
7	3	2	1	149·86	120·587	−180·126
8	7	3	2	123·05	124·337	78·385
9	7	3	4	141·44	116·672	77·585
10	1	2	3	146·56	121·122	−182·312
11	10	1	2	111·45	110·452	129·652
12	10	1	2	111·19	111·417	10·034
13	10	1	2	111·52	110·941	−110·811
14	2	1	10	109·59	115·613	−3·384
15	9	7	8	100·22	116·824	−20·770
16	9	7	8	100·02	116·064	−153·831
17	4	3	2	111·93	109·527	−119·338
18	4	3	2	111·59	110·919	124·161
19	5	4	3	109·05	116·060	−181·916
20	6	1	10	109·38	115·687	4·059
21	17	4	18	355·77	179·974	−48·663
22	21	17	4	151·86	101·772	−161·116
23	21	17	4	122·25	91·873	−35·116
24	21	17	4	111·06	75·397	86·473
25	22	21	23	110·82	110·479	159·597
26	22	21	23	110·96	109·592	−81·556
27	22	21	23	110·81	112·448	38·911

thermic. The calculated energetical barrier (about 335 kJ mol^{-1}) suggests, however, that process (A) → (B) will be extremely slow without further catalytic acceleration. This discovery does not seem to be surprising since our model system *Ia–II* still lacks any proton-transfer inclusion as in Eq. (*A*).

The interpretation of nuclear coordinates in (B) (Table II) enables to conclude that (B) is in fact an unexpected 3-aminocarbonyl-6-ethoxy-1,6-dihydropyridine (*III*) that issues from the sigmatropic addition of acetaldehyde (*Ia*) to 1,4-dihydropyridine ring of *II*.

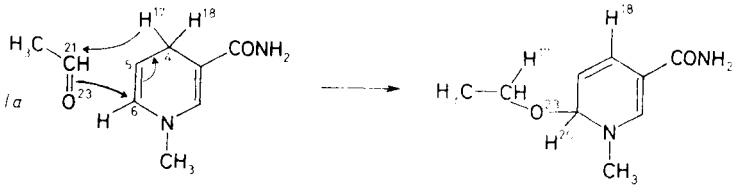

Ia *II* *III*

Some variations of electron distribution during process (A) → (B) are illustrated in Table III. The major changes take place where the reaction coordinate overcomes the energy barrier, i.e. near the $C_{21}...H_{17}$ distance 114 pm (point A_7). As expected the bond order $H_{17}—C_4$ has been gradually decreased to zero and the order for the created bond $C_{21}—H_{17}$ has been increased. Carbon center C_6 became positively charged while opposite changes of charge are observed for oxygen center O_{23}.

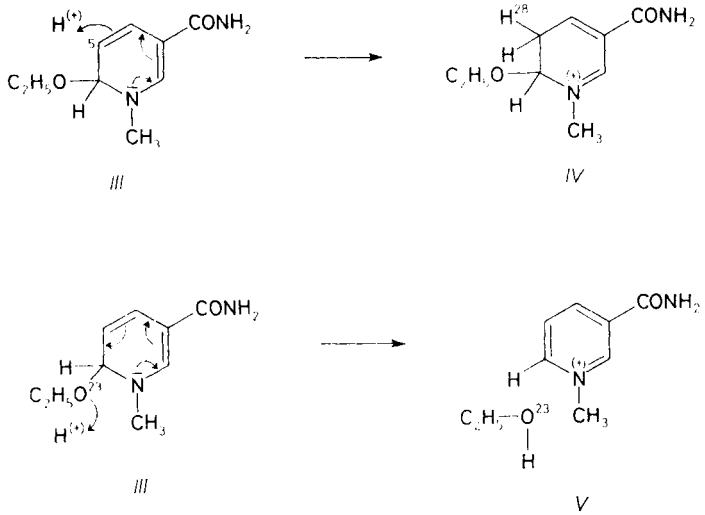

III *IV* *III* *V*

It is remarkable that the formation of 1,6-dihydropyridine intermediates like *III*, during the enzymatically catalyzed ethanol oxidation with NAD^+, has been considered by some authors[21]. Two possible courses of the second necessary stage of the transformation (*A*), i.e. the subsequent protonation of intermediate *III* were considered: C_5- and O_{23}-protonation of 1,6-dihydropyridine derivative *III*. The following approach was exploited: one proton was placed at a distance corresponding to the CH or OH bond length from the mentioned position C_5 or O_{23} and the systems were optimized with respect to all geometrical degrees of freedom. Two alternative MNDO models of product complex (C) and (D) were obtained in this way. Complex (C) was in fact 3-aminocarbonyl-6-ethoxy-1-methyl-5,6-dihydropyridinium (*IV*), in accord with the usual course of 1,6-dihydropyridines protonation[22,23]. On the other hand, complex (D) was found to be a supermolecule consisting of ethanol and 3-aminocarbonyl-1-methylpyridinium (*V*) components. Cation *V* is evidently our NAD model and hence the transformation (A) → (B) → (D) seems to be more adequate to approximate a possible biochemical path than the alternative four-step process (A) → (B) → (C) → (D).

Reaction of 1-Methyl-1,4-dihydronicotinamide with Protonated Acetaldehyde

The starting geometry of substrate complex (E) was obtained through MNDO optimization of supermolecule *Ib–II* using the same diastereoisomeric configuration as in the case of *Ia–II*. The interpretation of calculated nuclear coordinates (Table IV) has shown substantial differences between both substrate complexes (A) and (E). The strategy of MNDO energy calculations along the reaction coordinate was analogous to that in Fig. 3, using, however, steps 200, 180, 160, 140 and 120 pm and optimizing 77 geometrical degrees of freedom. After finding apparent energy minimum near point E_5 (Fig. 4) the reacting system was here once more optimized with respect to all 78 degrees of freedom to afford a product, complex (F), at 112 pm.

Fig. 4 shows that MNDO energy profile exhibits a similar maximum to that in Fig. 3 but at somewhat longer distance $C_{21}...H_{17}$ about 170 pm. Contrary to the process (A) → (B), in the case of (E) → (F) the calculated energetical barrier is sufficiently lower, only 89 kJ mol^{-1}, and the transformation is predicted to be strongly exothermic, the calculated enthalpy being about -90 kJ mol^{-1}. These results conclusively demonstrate the importance of substrate activation before its interaction with the coenzyme molecular part in accordance with the generally accepted role of BS in biocatalysis. From this point of view, the mechanism (A) → (B) → (D) seems to be less appropriate to interpret a correct biochemical path of acetaldehyde reduction with NADH in comparison with the more justified version (E) → (F). The changes of nuclear coordinates during the one-step process (E) → (F) are characterized by concerted elongation of the C_4—H_{17} bond and shortening of the $C_{21}...H_{17}$ distance. After overcoming the energy barrier the latter joint becomes the usual $C(sp^3)$–H

interaction in CH_2 group in the ethanol molecule. In addition, comparison of complexes (F) and (D) confirmed their marked similarity.

In Table V some variations of electron distribution during conversion (E) → (F) are given. As follows from MNDO charges the charge transfer from substrate *Ib* to 1,4-dihydropyridine ring of *II* is not achieved until the transition state and corresponding energetical barrier is surpassed. The phenomena are also reflected in the corresponding bond orders variations. Thus, the order of the created bond C_{21}—H_{17} has gradually been increased while that of the breaking one C_4—H_{17} has been decreased to zero. Process (E) → (F) is also accompanied by the continuous increase of hydroxyl bond order H_{28}—O_{23}.

Table II

Nuclear coordinates for optimal configuration of complex (B)

Atoms				Bond length, pm	Bond angle, °	Dihedral angle, °
I	J	K	L	J—I	K—J—I	L—K—J—I
2	1			139·05		
3	2	1		137·74	122·344	
4	3	2	1	145·64	119·030	0·722
5	4	3	2	135·50	120·188	−6·749
6	5	4	3	151·80	123·468	0·927
7	3	2	1	149·46	120·916	−177·992
8	7	3	2	122·98	124·431	67·892
9	7	3	4	141·72	116·535	65·286
10	1	2	3	146·86	119·440	−166·441
11	10	1	2	111·47	110·447	126·502
12	10	1	2	111·31	111·417	7·299
13	10	1	2	111·35	111·427	−112·973
14	2	1	10	109·75	116·270	12·513
15	9	7	8	100·27	116·363	−19·688
16	9	7	8	100·08	115·578	−151·034
17	4	3	2	314·95	87·644	−61·152
18	4	3	2	109·15	119·186	173·064
19	5	4	3	109·08	121·409	−181·017
20	6	1	10	113·21	107·510	43·953
21	17	4	18	111·88	115·387	−120·942
22	21	17	4	154·07	109·418	−151·543
23	21	17	4	140·63	112·982	−28·037
24	21	17	4	112·37	106·198	90·783
25	22	21	23	110·93	109·104	174·534
26	22	21	23	110·81	111·934	−66·293
27	22	21	23	110·82	112·071	55·293

TABLE III

Dependences of some MNDO net charges and bond orders on distance $C_{21}...H_{17}$ in supermolecule *Ia–II*

Centre	Point on reaction coordinate										
	A 356 pm	A_1 200 pm	A_2 180 pm	A_3 160 pm	A_4 140 pm	A_5 120 pm	A_6 116 pm	A_7 114 pm	*B* 112 pm	*C*	*D*
	Net atomic charges, e										
C_5	−0·172	−0·173	−0·173	−0·174	−0·176	−0·177	−0·176	−0·176	−0·214	−0·074	−0·093
C_6	0·080	0·080	0·081	0·082	0·086	0·093	0·095	0·096	0·378	0·316	0·164
H_{17}	0·003	−0·011	−0·011	−0·012	−0·006	0·002	0·005	0·004	0·000	−0·005	0·012
C_{21}	0·245	0·248	0·252	0·258	0·267	0·274	0·274	0·273	0·178	0·164	0·138
O_{23}	−0·296	−0·304	−0·311	−0·323	−0·350	−0·399	−0·412	−0·420	−0·367	−0·336	−0·365
Molecule *Ia*	0·000	−0·002	−0·007	−0·022	−0·057	−0·139	−0·164	−0·179	−0·171	−0·065	−0·203
	Bond orders										
H_{17}—C_4	0·979	0·972	0·931	0·948	0·931	0·831	0·807	0·791	0·006	0·004	0·001
H_{17}—C_{21}	0·004	0·103	0·153	0·229	0·338	0·497	0·534	0·557	0·977	0·978	0·980
O_{23}—C_6	0·000	0·014	0·021	0·033	0·068	0·082	0·089	0·095	0·977	1·022	0·003

After examining the rightward course of the Eq. (*I*) we tried to treat the opposite path connected with ethanol oxidation. Again two series of alternative calculations were performed describing interaction of 3-aminocarbonyl-1-methylpyridinium (*V*) with ethanol (*VIa*) and ethoxide (*VIb*). Components of these systems are shown in Fig. 5.

Reaction of 3-Aminocarbonyl-1-methylpyridinium with Ethanol

Starting supermolecule *V–VIa* (point *G*) is the equivalent of point *F* from the previous calculations. This supermolecule was transformed by shortening the distance

TABLE IV

Nuclear coordinates for optimal configuration of supermolecule *Ib–II* (E)

Atoms				Bond length, pm	Bond angle, °	Dihedral angle, °
I	J	K	L	J—I	K—J—I	L—K—J—I
2	1			139·66		
3	2	1		136·97	122·206	
4	3	2	1	151·32	122·039	0·533
5	4	3	2	150·09	111·696	1·402
6	5	4	3	135·32	123·602	−1·670
7	3	2	1	149·40	120·986	−178·694
8	7	3	2	124·31	124·138	101·081
9	7	3	4	139·07	117·463	104·904
10	1	2	3	147·16	121·504	−179·380
11	10	1	2	111·37	110·500	118·381
12	10	1	2	111·16	111·157	−1·587
13	10	1	2	111·40	110·086	−121·323
14	2	1	10	109·69	115·829	1·280
15	9	7	8	99·91	120·453	16·763
16	9	7	8	99·85	119·267	−195·896
17	4	3	2	111·74	110·253	−120·055
18	4	3	2	111·63	110·314	123·383
19	5	4	3	109·08	116·140	−181·736
20	6	1	10	109·36	115·914	−0·991
21	17	4	18	445·76	233·043	−77·075
22	21	17	4	150·71	85·752	−158·096
23	21	17	4	128·38	120·237	−36·460
24	21	17	4	110·70	64·954	76·630
25	22	21	23	110·95	109·463	151·295
26	22	21	23	111·41	108·416	−90·848
27	22	21	23	110·92	113·353	29·477
28	23	21	24	96·11	119·257	−4·641

$H_{17}...C_4$ starting from 300 pm (point G_1 on the reaction path) and after every step the reacting system was optimized with respect to other degrees of freedom, except the fixed distance. Fig. 6 shows that the energy of the system gradually increases up to the value of the fixed distance near 118 pm (point G_7) and then steeply falls to a minimum of about 112 pm. Final point *H* was obtained by optimizing all 78 degrees of freedom. The resulting optimal nuclear configuration (H) is practically the same as (E) from the previous calculation, composed from molecules *II* and *Ib*. The calculated apparent activation energy amounts to 186 kJ mol^{-1}, being higher than for the (E) → (F) process. This indicates that our calculations approximated the transition states by two different saddlepoints. The enthalpy for the (G) → (H) process results practically the same as for (E) → (F), but with the opposite sign. In Table VI some variations of electron distribution during (G) → (H) conversion are given.

Reaction of 3-Aminocarbonyl-1-methylpyridinium with Ethoxide

The starting geometry (point *I*) of this reaction path was obtained by optimizing the supermolecule *V*—*VIb* with respect to all 75 degrees of freedom. The interpretation of nuclear coordinates led us to the conclusion that point *I* is in fact dihydropyridine *III*. Comparison of complexes (B) and (I) confirmed their marked similarity. Starting from point *I* the distance $H_{17}...C_4$ was stepwise shortened and all the other degrees of freedom optimized. The energy profile of this process (Fig. 7) exhibits its maximum near 118 pm (point I_8). Calculated energy barrier (338 kJ mol^{-1}) is almost the same as for the (A) → (B) process, the enthalpy change is negligible. Relatively high energetical barrier is probably the reason why although reactions like $V + C_2H_5O^- \rightarrow III$

TABLE V
Dependence of MNDO charges and bond orders on distance $C_{21}...H_{17}$ in supermolecule *Ib*–*II*

Point on reaction coordinate	Total charge		Bond orders		
	II	*Ib*	H_{17}—C_4	H_{17}—C_{21}	H_{28}—O_{23}
E 446 pm	0·001	0·999	0·978	0·000	0·939
E_1 200 pm	0·042	0·958	0·943	0·185	0·940
E_2 180 pm	0·078	0·922	0·924	0·259	0·941
E_3 160 pm	0·215	0·785	0·842	0·432	0·945
E_4 140 pm	0·983	0·017	0·000	0·972	0·970
E_5 120 pm	1·010	−0·010	0·000	0·978	0·972
F 112 pm	1·012	−0·012	0·000	0·981	0·972

have been observed for certain quaternary pyridinium salts with alcoholates in appropriate alcohol solutions (e.g. refs[24-26]), no spontaneous decomposition of compounds type *III* to aldehydes and *II* was observed. Complete optimization of the final point *J* led to supermolecule *Ia–II*. Some variations of electron distribution

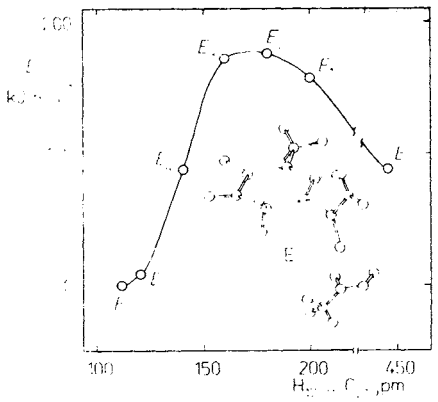

FIG. 4

Dependence of MNDO energy on distance between centres H_{17} and C_{21} in supermolecule *Ib-II*

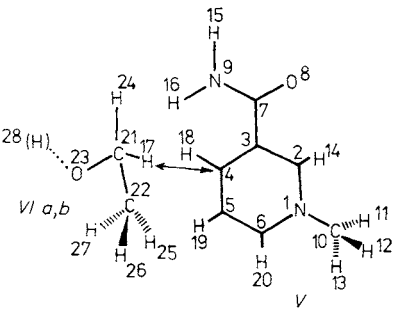

FIG. 5

Numbering of the studied system *V–VIa,b*. *V* 3-aminocarbonyl-1-methylpyridinium, *VIa* ethanol, *VIb* ethoxide anion

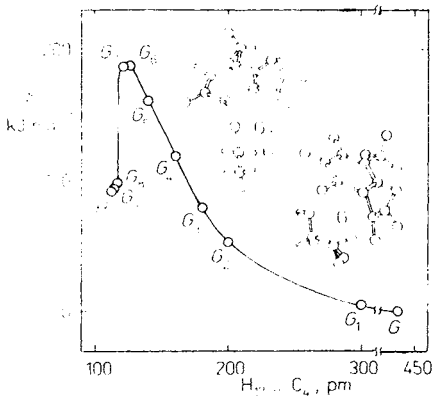

FIG. 6

Dependence of MNDO energy on distance between centres H_{17} and C_4 in supermolecule *V–VIa*

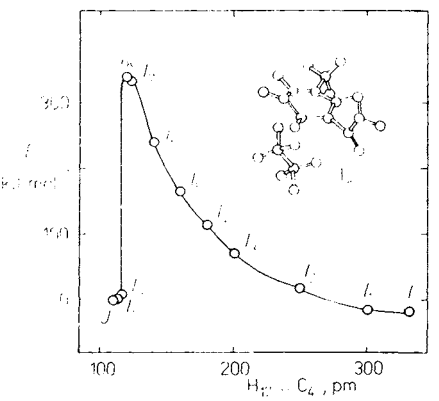

FIG. 7

Dependence of MNDO energy on distance between centres H_{17} and C_4 in supermolecule *V–VIb*

TABLE VI

Dependence of some MNDO net charges and bond orders on distance $H_{17}...C_4$ in supermolecule *V–VIa*

Centre	Point on reaction coordinate										
	G 436 pm	G_1 300 pm	G_2 200 pm	G_3 180 pm	G_4 160 pm	G_5 140 pm	G_6 120 pm	G_7 118 pm	G_8 116 pm	G_9 114 pm	*H* 112 pm
	net atomic charges, e										
C_4	0·136	0·137	0·152	0·168	0·198	0·253	0·230	0·224	0·128	0·128	0·129
C_{21}	0·137	0·143	0·154	0·158	0·170	0·230	0·363	0·367	0·440	0·440	0·440
C_{23}	−0·365	−0·365	−0·355	−0·353	−0·346	−0·285	−0·177	−0·170	−0·084	−0·084	−0·085
Molecule *VIa*	0·000	0·000	0·006	0·016	0·048	0·263	0·596	0·622	0·983	0·986	0·987
	Bond orders										
$H_{17}—C_4$	0·000	0·013	0·116	0·176	0·274	0·491	0·818	0·833	0·976	0·977	0·978
$H_{17}—C_{21}$	0·981	0·980	0·976	0·960	0·933	0·816	0·483	0·462	0·000	0·000	0·000
$H_{28}—O_{23}$	0·972	0·971	0·969	0·968	0·966	0·963	0·948	0·957	0·940	0·940	0·940
$O_{23}—C_{21}$	0·988	0·990	0·994	0·996	1·000	1·040	1·154	1·162	1·250	1·250	1·250

TABLE VII

Dependence of some MNDO net charges and bond orders on distance $H_{17}...C_4$ in supermolecule *V–VIb*

Centre	Point on reaction coordinate											
	I 330 pm	I_1 300 pm	I_2 250 pm	I_3 200 pm	I_4 180 pm	I_5 160 pm	I_6 140 pm	I_7 120 pm	I_8 118 pm	I_9 116 pm	I_{10} 114 pm	*J* 112 pm
						Net atomic charges, e						
C_4	0·056	0·056	0·054	0·053	0·056	0·069	0·092	0·129	0·141	0·120	0·122	0·123
C_{21}	0·176	0·171	0·161	0·149	0·132	0·122	0·108	0·103	0·114	0·246	0·248	0·248
C_{23}	−0·362	−0·361	−0·352	−0·354	−0·349	−0·346	−0·345	−0·330	−0·325	−0·294	−0·298	−0·299
Molecule *VIb*	−0·170	−0·170	−0·165	−0·174	−0·186	−0·165	−0·157	−0·117	−0·108	0·000	0·000	0·000
						Bond orders						
$H_{17}—C_4$	0·004	0·000	0·028	0·096	0·143	0·236	0·378	0·645	0·732	0·975	0·977	0·978
$H_{17}—C_{21}$	0·976	0·977	0·977	0·973	0·966	0·948	0·900	0·730	0·642	0·000	0·000	0·000
$C_{23}—C_{21}$	0·974	0·974	0·991	0·976	0·979	0·980	0·988	1·025	1·055	1·402	1·401	1·401
$C_{23}—C_6$	0·977	0·977	0·978	0·976	0·972	0·972	0·960	0·923	0·891	0·000	0·000	0·000

during (I) → (J) process are illustrated in Table VII. Evolution of bond order O_{23}--C_6 along the reaction path may be of interest: at point I_8 it still amounts to 0·891, at the following point I_9 the bond order is zero.

CONCLUSIONS

The proposed concept of the CMEC may contribute to unify considerations regarding the physico-chemical signification of different quantum chemical calculations being performed in biocatalysis on elementary reaction steps. The CMEC concept can be applied on different levels of sophistication using standard MO methods and so enables to understand various micromechanistic details in enzymatic processes not available from current experiments by relatively simple means. Independently to our CMEC interpretations two novel theoretical treatments on biocatalytic effects have been published recently[27,28].

Stamato et al.[27] have studied a large system of serine proteinase calculating the active site quantum mechanically while expressing the substrate interaction with surrounding protein by minimization of van der Waals contacts. This treatment may be in fact considered to be a more sophisticated CMEC. On the other hand, Warshel and Sussman[28] have suggested that an enzymatically reacting system may be driven toward transition state by gradual change of the calculated charge distribution. The reported calculations of chymotrypsin[28] are based on a combination of the empirical VB method and a free energy perturbation procedure.

Using a very simple version of the CMEC, involving trivial models of C and BS, the importance of pre-activation of a substrate before its interaction with a coenzyme is demonstrated in the special case of enzymatic acetaldehyde reduction with NADH.

REFERENCES

1. Bolis G., Ragazzi M., Salvaderi D., Ferro D. R., Clementi E.: Gazz. Chim. Ital. *108*, 425 (1978).
2. Clementi E., Ranghino G., Scordamaglia R.: Chem. Phys. Lett. *49*, 218 (1977).
3. Náray-Szabó G., Surján P. R.: Theochem, J. Mol. Struct. *123*, 85 (1985).
4. Nakagawa S., Umeyama H.: J. Theor. Biol. *96*, 473 (1982).
5. Umeyama H., Nakagawa S., Nomoto T.: Chem. Pharm. Bull. *28*, 2874 (1980).
6. Tapia O., Eklund H., Bränden C. I. in: *Steric Aspects of Biomolecular Interactions* (G. Náray-Szabó and K. Simin, Eds). CRC Press, Florida 1986.
7. Tapia O., Andres J., Aullo J. M., Bränden C. I.: J. Chem. Phys. *83*, 4673 (1985).
8. Tapia O., Eklund H.: Enzyme *36*, 101 (1986).
9. Eklund H., Samana J. P., Wallén L., Bränden C. I., Åkeson Å., Jones T. A.: J. Mol. Biol. *146*, 561 (1981).
10. Dewar M. J. S., Storch D. M.: Proc. Natl. Acad. Sci. U.S.A. *82*, 2225 (1985).
11. Dewar M. J. S., Thiel W.: J. Am. Chem. Soc. *99*, 4899 (1977).
12. Fletcher R., Powell M. J. D.: Comput. J. *6*, 163 (1963).
13. Davidon W. C.: Comput. J. *10*, 406 (1986).

14. Ferreira R., Gomes M. A. F.: Int. J. Quantum Chem. *22*, 537 (1982).
15. Krechl J., Kuthan J.: Int. J. Quantum Chem. *21*, 1029 (1982).
16. Krechl J., Kuthan J.: Int. J. Quantum Chem. *24*, 479 (1983).
17. Krechl J., Kuthan J.: Theochem, J. Mol. Struct. *170*, 239 (1988).
18. Krechl J., Kuthan J.: Collect. Czech. Chem. Commun. *48*, 484 (1983).
19. Krechl J., Kuthan J.: Collect. Czech. Chem. Commun. *46*, 740 (1981).
20. Krechl J., Kuthan J.: Collect. Czech. Chem. Commun. *45*, 2187 (1980).
21. Bruice T. C., Benkovic S. J.: *Bioorganic Mechanisms*, Vol. II, p. 301. Benjamin, New York 1966.
22. Eisner U., Kuthan J.: Chem. Rev. *72*, 1 (1972).
23. Kuthan J., Kurfürst A.: Ind. Eng. Chem., Prod. Res. Develop. *21*, 191 (1982).
24. Ohnishi Y., Kitami M.: Tetrahedron Lett. *1978*, 4035.
25. Kuthan J., Krechl J., Bělchradský M., Tříska P.: Collect. Czech. Chem. Commun. *49*, 597 (1984).
26. Kaválek J., Lyčka A., Macháček V., Štěrba V.: Collect. Czech. Chem. Commun. *40*, 1166 (1975).
27. Stamato F. M. L. G., Longo E., Ferreira R., Tapia O.: J. Theor. Biol. *118*, 45 (1986).
28. Warshel A., Sussman F.: Proc. Natl. Acad. Sci. U.S.A. *83*, 3806 (1986).

Translated by the author (J. Krechl).